Organic Process Research & Development **2006**, *10,* 1219–1226

# Monitoring of Solvent-Mediated Polymorphic Transitions Using in Situ Analysis Tools

Ryo Kobayashi,*,† Yasuto Fujimaki,‡ Tatsuzo Ukita,† and Yukio Hiyama‡

*Process Chemistry Research Laboratories, Tanabe Seiyaku Co., Ltd., 16-89, Kashima 3-chome, Yodogawa-ku, Osaka 532-8505, Japan, and Division of Drugs, National Institute of Health Sciences, 1-18-1, Kamiyoga, Setagaya-ku, Tokyo 158-8501, Japan*

**Abstract:**

**In general, polymorphs have been identified by using off-line techniques such as X-ray diffraction, Raman spectroscopy, and infrared spectroscopy (IR). However, these techniques are unsuitable for process monitoring because they are slow and require sample preparation. In this study, the possibility of applying in situ techniques to the monitoring of solvent-mediated transitions was investigated. These in situ techniques include Raman spectroscopy, near-infrared spectroscopy (NIR), and focused beam reflectance measurement (FBRM), in which it is possible to perform measurements quickly and in a nondestructive manner. Raman spectroscopy is effective as a process analytical technology (PAT) tool for determining polymorphic transition because this technique is insensitive to aqueous solvents. NIR can be used for measurements on crystal polymorphs with sampling from a slurry; however, it is not effective if it is also off-line due to the interruption of the absorption band of water. Providing the particle size changes with the polymorphic transition, FBRM can be very useful as a PAT tool for monitoring not only particle distribution size but also polymorphic transition. Raman spectroscopy provides an insight into the properties of crystallization, especially the rapid quantitative analysis of polymorphic transition. This technique offers a time-saving approach for the development of the crystallization process. In situ techniques such as Raman spectroscopy can be used during scale-up to understand and monitor crystallization processes.**

## Introduction

Crystallization from solution is well established as an essential separation and purification technique for active pharmaceutical ingredients (APIs). However, the presence of multiple crystal polymorphs of the compound is a problem that is frequently encountered in the pharmaceutical industry. The phenomenon of polymorphic transition frequently affects various pharmaceutical characteristics such as stability,[1] solubility,[2] bioavailability,[3] and the purification effect. It is important to gain an understanding of this phenomenon in the pharmaceutical manufacturing process. However, it is difficult to find general rules for polymorphism control in crystallization. Therefore, it is effective that the monitoring of this phenomenon simultaneously requires the understanding of the kinetics of polymorphic transition.

In industry, polymorphic transition in a slurry is generally confirmed by differential scanning calorimetry (DSC), X-ray powder diffraction (XRPD), infrared spectroscopy (IR), near-infrared spectroscopy (NIR),[4] or Raman spectroscopy. However, these conventional methods require time for sample preparation or measurement. Therefore, they are employed as off-line analysis tools for materials rather than real-time monitoring systems.[5]

The *Guidance for Industry PAT-A Framework for Innovative Pharmaceutical Development, Manufacturing, and Quality Assurance* was issued by the U.S. Food and Drug Administration (FDA) in 2004.[6] The application of process analytical technology (PAT) is currently an area of high interest.[7] Several in-line analytical techniques such as FT-IR,[8−10] NIR,[11] Raman spectroscopy,[12−14] and FBRM[15−16] have been employed as PAT tools for understanding and monitoring crystallization processes. These techniques have attracted

* Corresponding author. Telephone: +81-6-6300-2838 (ext. 716-2838). Fax: +81-6-6300-2816. E-mail: ryo-koba@tanabe.co.jp.

† Process Chemistry Research Laboratories, Tanabe Seiyaku Co., Ltd.

‡ Division of Drugs, National Institute of Health Sciences.

(1) Lewis, N. *Org. Process Res. Dev.* **2000**, *4*, 407−412.

(2) Chemburkar, S. R.; Bauer, J.; Deming, K.; Spiwek, H.; Patel, K.; Morris, J.; Henry, R.; Spanton, S.; Dziki, W.; Porter, W.; Quick, J.; Bauer, P.; Donaubauer, J.; Narayanan, B. A.; Soldani, M.; Riley, D.; McFarland, K. *Org. Process Res. Dev.* **2000**, *4*, 413−417.

(3) Aguiar, A. J.; Krc, J.; Kinkel, A. W.; Samyn J. C. *J. Pharm. Sci.* **1967**, *56*, 847.

(4) Aaltonen, J.; Rantanen, J.; Siiria, S.; Karjalainen, M.; Jorgensen, A.; Laitinen, N.; Savolainen, M.; Seitavuopio, P.; Louhi-Kultanen, M.; Yliruusi, J. *Anal. Chem.* **2003**, *75*, 5267−5273.

(5) Threlfall, T. L. *Analyst (Cambridge, United Kingdom*) **1995**, *120*, 2435−2460.

(6) *FDA Guidance for Industry: PAT - A Framework for Innovative Pharmaceutical Development, Manufacturing, and Quality Assurance*; Office of Training and Communication, Division of Drug Information, HFD-240, Center for Drug Evaluation and Research, Food and Drug Administration, Rockville, MD, September 29, 2004.

(7) Birch, M.; Fussell, S. J.; Higginson, P. D.; McDowall, N.; Marziano, I. *Org. Process Res. Dev.* **2005**, *9*, 360−364.

(8) Liotta, V.; Sabesan, V. *Org. Process Res. Dev.* **2004**, *8*, 488−494.

(9) Horvath, A.; De Smet, K.; Ormerod, D.; Depre, D.; Perez-Balado, C.; Govaerts, T.; Van den Heuvel, D.; Schorpion, I. *Org. Process Res. Dev.* **2005**, *9*, 356−359.

(10) Pollanen, K.; Hakkinen, A.; Reinikainen, S. P.; Rantanen, J.; Karjalainen, M.; Louhi-Kultanen, M.; Nystrom, L. *J. Pharm. Biomed. Anal.* **2005**, *38*, 275−284.

(11) De Smet, K.; van Dun, J.; Stokbroekx, B.; Spittaels, T.; Schroyen, C.; Van Broeck, P.; Lambrechts, J.; Van Cleuvenbergen, D.; Smout, G.; Dubois, J.; Horvath, A.; Verbraeken, J.; Cuypers, J. *Org. Process Res. Dev.* **2005**, *9*, 344−347.

(12) Starbuck, C.; Spartalis, A.; Wai, L.; Wang, J.; Fernandez, P.; Lindemann, C. M.; Zhou, G. X.; Ge, Z. *Cryst. Growth Des.* **2002**, *2*, 515−522.

(13) Hu, Y.; Liang, J. K.; Myerson, A. S.; Taylor, L. S. *Ind. Eng. Chem. Res.* **2005**, *44*, 1233−1240.

(14) Wang, F.; Wachter, J. A.; Anrose, F. J.; Berglund K. A. *Org. Process Res. Dev.* **2000**, *4*, 391−395.

(15) O'Sullivan, B.; Barrett, P.; Hsiao, G.; Carr, A.; Glennon, B. *Org. Process Res. Dev.* **2003**, *7*, 977−982.

(16) O'Sullivan, B.; Glennon, B. *Org. Process Res. Dev.* **2005**, *9*, 884−889.

10.1021/op060046y CCC: $33.50 
Published on Web 09/21/2006

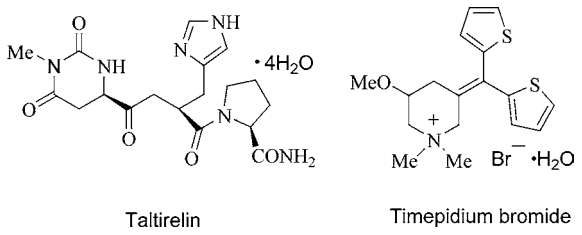


***Figure 1.*** **Structures of taltirelin and timepidium bromide.**

attention as quick and nondestructive methods. In recent years, several groups[12,13,17−19] have explored the use of in-line Raman spectroscopy to monitor polymorphic transition in a slurry from the viewpoint of understanding and monitoring the kinetics of the transition. NIR spectroscopy has been described as a useful tool in the monitoring of the reaction[20,21] and drying[22] processes. However, the application of polymorphic transition monitoring for aqueous solution was scarcely addressed in these works.[23] Moreover, the analysis of NIR spectroscopy has needed a spectrum preprocessing or a complicated multivariate analysis. FBRM has been used for particle analysis in the crystallization process. If a polymorphic transition is accompanied by a change in the crystal habit, the dramatic changes will result in a shape of the particle distribution that is measurable by FBRM.

In this work, the simple applications of NIR, Raman spectroscopy, and FBRM to the in situ analysis of solvent-mediated polymorphic transition were compared.

## Materials and Methods

**Materials.** *Taltirelin.* Taltirelin[24,25] (Figure 1): (−)-*N*-[(*S*)-hexahydro-1-methyl-2,6-dioxo-4-primidinylcarbonyl]-L-histidyl-L-prolinamide tetrahydrate, obtained from Tanabe Seiyaku Co., Ltd., has two known crystal forms (α- and *β*-forms). The α-form, which exhibits good solid−liquid separation characteristics, is selected as the API. The problem is that α-form crystals undergo a transformation into the thermodynamically more stable *β*-form by a solvent-mediated polymorphic transition. In order to ensure the desired polymorphism, it is necessary to detect the start of the polymorphic transition.

The *β*-form is prepared by a solvent-mediated transition from the α-form in an aqueous solution at 10 °C. The two forms can be distinguished by XRPD (Mac science and MXP3VA). Furthermore, it is also possible to calculate the content ratio of the α-form by using the intensity of the 16.2°/2*θ* peak. (The minimum detection limit was 5%.)

**Materials.** *Timepidium Bromide.* Timepidium bromide (Figure 1): 3-(di-2-thienylmethylene)-5-methoxy-1,1-dimethylpiperidium bromide, obtained from Tanabe Seiyaku Co., Ltd., has three known hydrate forms (anhydrate, monohydrate, and dihydrate). The *β*-form (monohydrate), which has good chemical stability, is selected as the API. Although both the α-form (dihydrate) and *β*-form (monohydrate) are obtained by recrystallization from an aqueous solution, the α-form transforms into the *β*-form upon prolonged stirring. In order to ensure consistent production of the *β*-form, it is necessary to monitor the complete conversion of the α-form.

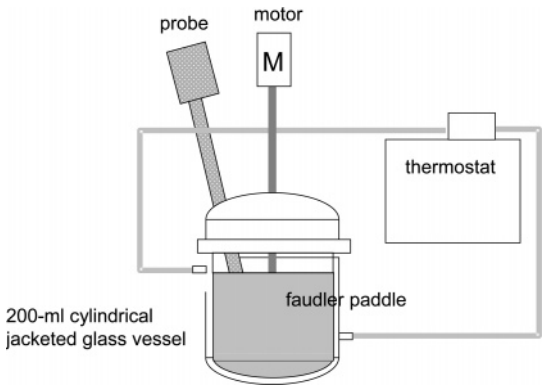


***Figure 2.*** **Schematic diagram of experimental apparatus for polymorphic transition.**

**Methods.** *Experimental Conditions.* All the compounds were respectively from the same batches and were used without carrying out further purification.

The slurry of the metastable crystal was adjusted to conditions that facilitate the investigation of a solvent-mediated polymorphic transition, which was initiated by seeding of the stable form. The experimental scale was changed according to the analysis equipment (probe size, etc.). The typical procedure and scale of experiment are described as follows.

**Methods.** *Taltirelin.* The experimental apparatus is shown in Figure 2. Water (150 mL) was placed in a 200-mL cylindrical, jacketed, glass vessel equipped with a Pfaudler paddle, and the inner temperature was maintained at 10 °C. Taltirelin (α-form; 60 g) was then added. This system was stirred isothermally for several hours. During the stirring period, a polymorphic transition was initiated by seeding of the *β*-form (600 mg) and observed by in situ monitoring with Raman, NIR spectroscopy, and FBRM.

Under these conditions, the solubility of taltirelin is 15.1 g/100 mL for the α-form and 8.5 g/100 mL for the *β*-form.

**Methods.** *Timepidium Bromide.* A 150-mL portion of solvent (water containing 10 w/w% acetone) was placed in the above-mentioned 200-mL glass vessel, and the inner temperature was maintained at 20 °C. Timepidium bromide (α-form; 15 g) was then added. This system was stirred isothermally for several hours. During the stirring period, polymorphic transition was initiated by seeding of the *β*-form (300 mg), and observed using the same three methods as above.

Under these conditions, the solubility of timepidium bromide is 3.4 g/100 mL for the α-form and 2.5 g/100 mL for the *β*-form.

**Instruments.** *1. Raman Spectroscopy.* Raman spectra were recorded using a RamanRxn1 Analyzer (Kaiser Optical Systems Inc., U.S.A) equipped with a fiber-optic probe, using

(17) Ono, T.; ter Horst, J. H.; Jansens, P. J. *Cryst. Growth Des.* **2004**, *4*, 465−469.
(18) Ono, T.; Kramer, H. J. M.; ter Horst, J. H.; Jansens, P. J. *Cryst. Growth Des.* **2004**, *4*, 1161−1167.
(19) Caillet, A.; Puel, F.; Fevotte, G. *Int. J. Pharm.* **2006**, *307*, 201−208.
(20) Bjorsvik, H. R. *Org. Process Res. Dev.* **2004**, *8*, 495−503.
(21) Bird, P. A.; Sharp, D. C. A.; Woodley, J. M. *Org. Process Res. Dev.* **2002**, *6*, 569−576.
(22) Green, R. L.; Thurau, G.; Pixley, N. C.; Mateous, A.; Reed, R. A.; Higgins, J. P. *Anal. Chem.* **2005**, *77*, 4515−4522.
(23) Norris, T.; Aldridge, P. K.; Sekulic, S. S. *Analyst (Cambridge, United Kingdom)* **1997**, *122*, 549−552.
(24) Maruyama, S.; Ooshima, H.; Kato, J. *Chem. Eng. J.* **1999**, *75*, 193−200.
(25) Maruyama, S.; Ooshima, H. *J. Cryst. Growth* **2000**, *212*, 239−245.

an approximately 250-mW, 785-nm laser excitation. The acquisition conditions were optimized so that each spectrum was captured with an exposure time of 10 s with four accumulations in the case of taltirelin and an exposure time of 2 s with three accumulations for timepidium bromide.

A quantitative analysis was performed using the partial least-squares (PLS) regression method (Holo React).

*2. NIR Spectra Acquisition.* All near-infrared spectra were measured with an MPA system (Bruker Optics K.K., Tokyo, Japan) equipped with a fiber-optic module. The instrument was controlled with OPUS ver. 5.0 (Ettlingen, Germany), which also processed the spectral data. All samples were analyzed with the MPA by using the fiber-optic probe. This probe was set into a stirred reactor containing the slurry. The measurements were collected over the range of 12000−4000 $cm^{-1}$ with the spectral resolution set at 8 $cm^{-1}$, and each spectrum was taken as an average of 128 scans (1 spectra = the average of 128 scans).

A quantitative analysis was performed on the raw absorbance data using the partial least-squares (PLS) regression method (OPUS ver. 5.0).

In order to remove the influence of segregation in the slurry, an analytical curve was created using the data set which measured five spectra per sample (one concentration).

*3. FBRM.* Focused beam reflectance measurement was performed with an FBRM: D-600L manufactured by Mettler Toledo, U.S.A. The instrument is equipped with a low-level laser light. When the laser light intersects a particle, it begins to backscatter. This backscattering continues until the opposite edge of the particle is reached. The duration of backscattering is converted into a distance known as the chord length.[26] The chord length distribution is then obtained from these values. In this experiment, the FBRM probe has a measurement range of 1−1000 $\mu$m, and the measurement duration was set at 30 s.

All probes (Raman, NIR, FBRM) were not installed in the shown reactor. Each probe was set, and data were collected by repeating the reaction. However, all measurements used samples from the same batch.

## Results and Discussion

**A. Crystal Form Monitoring by Raman and NIR Spectroscopy.** *A.1. Raman Spectroscopy. A.1.1. Analysis of Taltirelin.* Raman spectra of taltirelin (α- and $\beta$-forms in slurry) are shown in Figure 3a. The spectrum form changes in the region of around 1100−400 $cm^{-1}$ according to the polymorphic ratios of the crystals in the slurry. The changes were comparatively large in the region of 600−550 $cm^{-1}$. The peak at 555 $cm^{-1}$ was confirmed to be due to the stable crystal form. The intensity of this peak increases as the polymorphic transition progressed (Figure 3, b and c); the changes were confirmed to be readily detectable because this peak was not obscured by water peaks. In fact, by using this peak, it was possible to monitor the trend of the spectral changes accompanying the polymorphic transition in the slurry.

*A.1.2. Analysis of Timepidium Bromide.* The Raman spectra changed in proportion to the polymorphic ratio in the slurry (Figure 4a). In order to demonstrate the applicability of Raman spectroscopy to the quantitative characterization of the polymorphs, a calibration curve was constructed. Five binary mixtures of the two forms were prepared by simple weight fraction; these were used to build a calibration curve by PLS regression analysis. The calculation results for the 900−400 $cm^{-1}$ range showed a strong correlation (determination coefficient ($R^2$) = 98.8%; number component: 1) between the intensity and the spectral changes (Figure 4b). In this manner, the method of identifying the polymorphic type by Raman spectroscopy was confirmed.

In the case of in situ measurements in a slurry, it is observed that a reduction in peak intensity at 578 $cm^{-1}$ and an increase in peak intensity at 586 $cm^{-1}$ (Figure 4c) occur during the transition. These peaks could be attributed to the

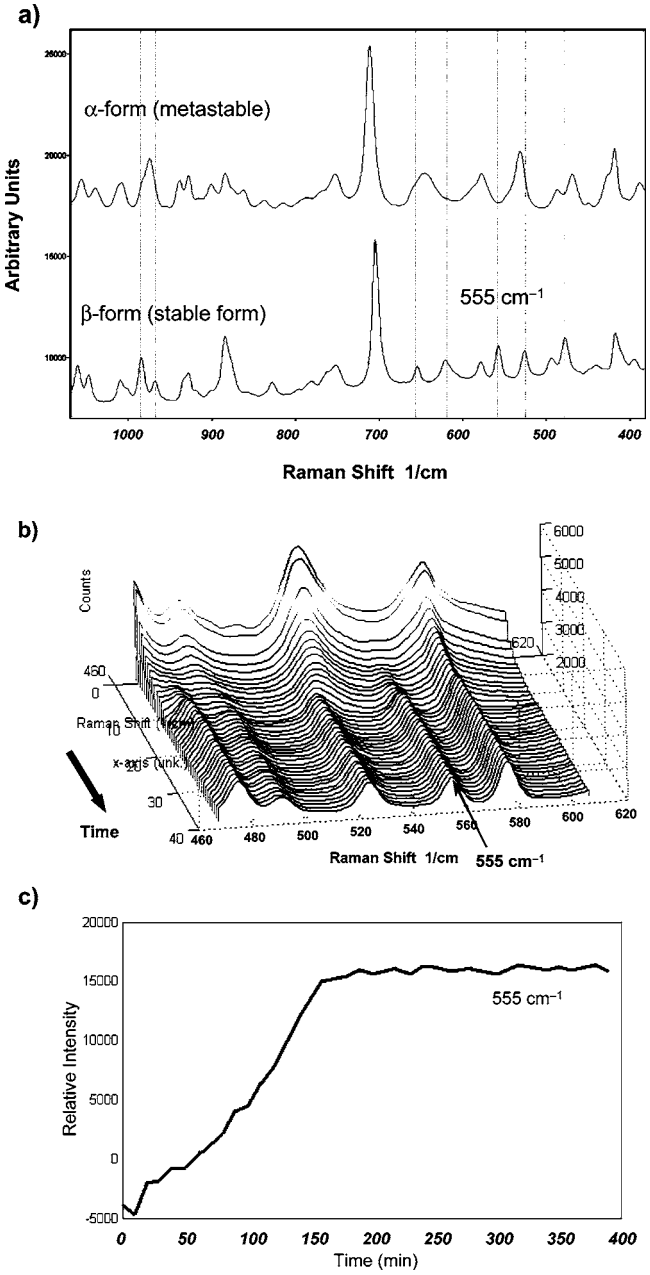


***Figure 3.*** **(a) Raman spectra of α- and $\beta$-forms of taltirelin at 1100−400 $cm^{-1}$. (b) Waterfall plot (600−450 $cm^{-1}$). (c) Relative intensity profile (555 $cm^{-1}$ peak).**

(26) Pearson, A. P.; Glennon, B.; Kieran, P. M. *Biotechnol. Prog.* **2003**, *19*, 1342−1347.

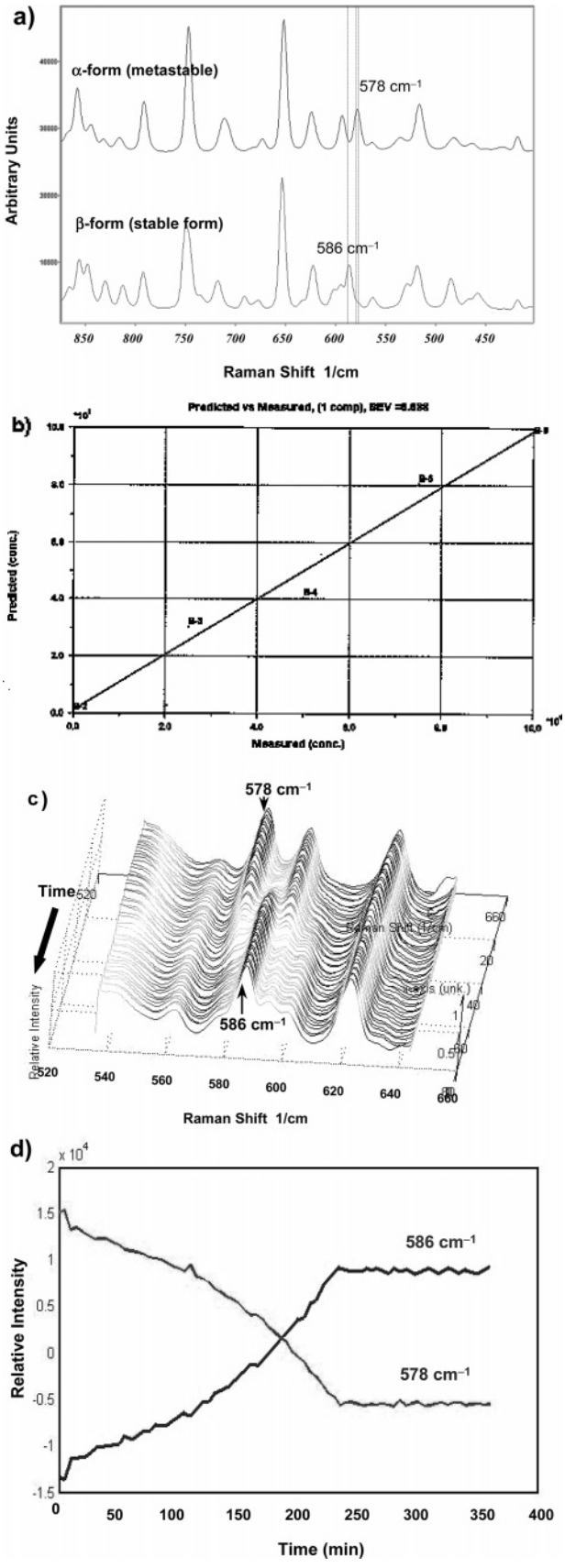


***Figure 4.*** **(a) Raman spectra of α- and *β*-forms of timepidium bromide at 900−400 cm$^{-1}$. (b) Analytical curve of Raman spectra of timepidium bromide (powder) in the region of 900−400 cm$^{-1}$. Determination coefficient ($R^2$) was 98.8% (RMSECV = 6.69, rank = 1). (c) Waterfall plot (660−520 cm$^{-1}$). (d) Relative intensity profile (586, 578 cm$^{-1}$ peaks).**

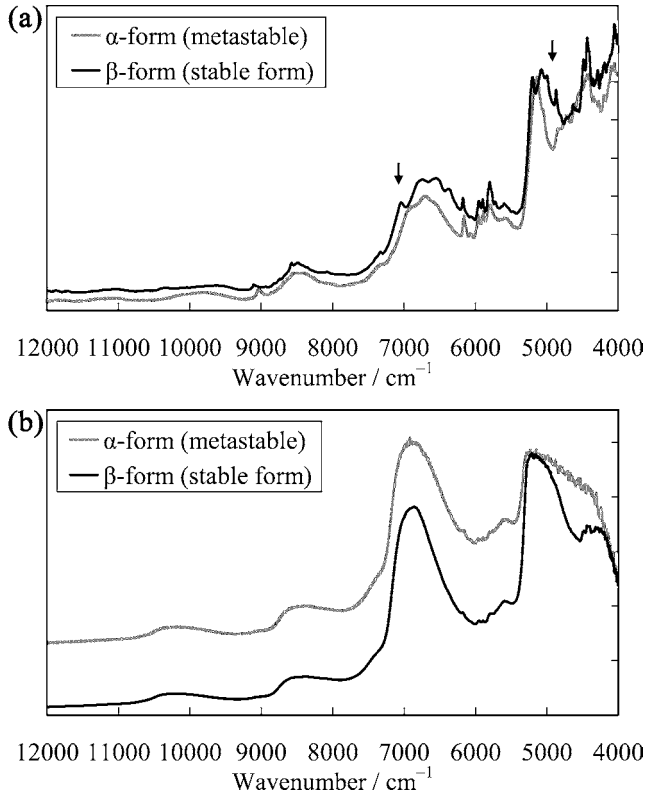


***Figure 5.*** **(a) NIR spectra of taltirelin (powder) in the region of 12000−4000 cm$^{-1}$. (b) NIR spectra of taltirelin in slurry in the region of 12000−4000 cm$^{-1}$.**

metastable form (578 cm$^{-1}$) and the stable form (586 cm$^{-1}$), as shown in Figure 4a. Therefore, the changes in peak intensities shown in Figure 4d indicate the polymorphic transition of timepidium bromide.

Raman spectroscopy is considered to be an effective monitoring tool of polymorphic transition in a slurry because it can monitor the changes in the crystal habit accompanying the polymorphic transition without the interference of water peaks.

*A.2. NIR Spectra Acquisition. A.2.1. Analysis of Taltirelin.* NIR spectra of taltirelin (powder) are shown in Figure 5a. Changes in some specific spectral shapes (7000 and 5000 cm$^{-1}$ neighborhoods) are observed in each spectrum. It was considered that the NIR spectra were influenced by a change in the molecular structure accompanied by the rotation of the amide bonding in the polymorphic transition of taltirelin.[24] In fact, this region is equivalent to the second overtone and combinations of the amide bonding, and these specific peaks can be used to identify the polymorphs.

Figure 5b shows the NIR spectra of taltirelin in the slurry. The entire region of the spectrum is covered by absorption bands of water (6900 cm$^{-1}$/first overtone and 5200 cm$^{-1}$/combinations), and the peaks corresponding to Taltirelin are completely hidden. Thus, in a slurry, the α- and *β*-forms cannot be distinguished on the basis of their specific peaks. It was considered that the identification of the crystal form in the slurry is difficult owing to the interference of these absorption bands by water. However, in the case of a highly concentrated slurry, where the water bands are weaker, the identification of the crystal form is possible such as in Figure

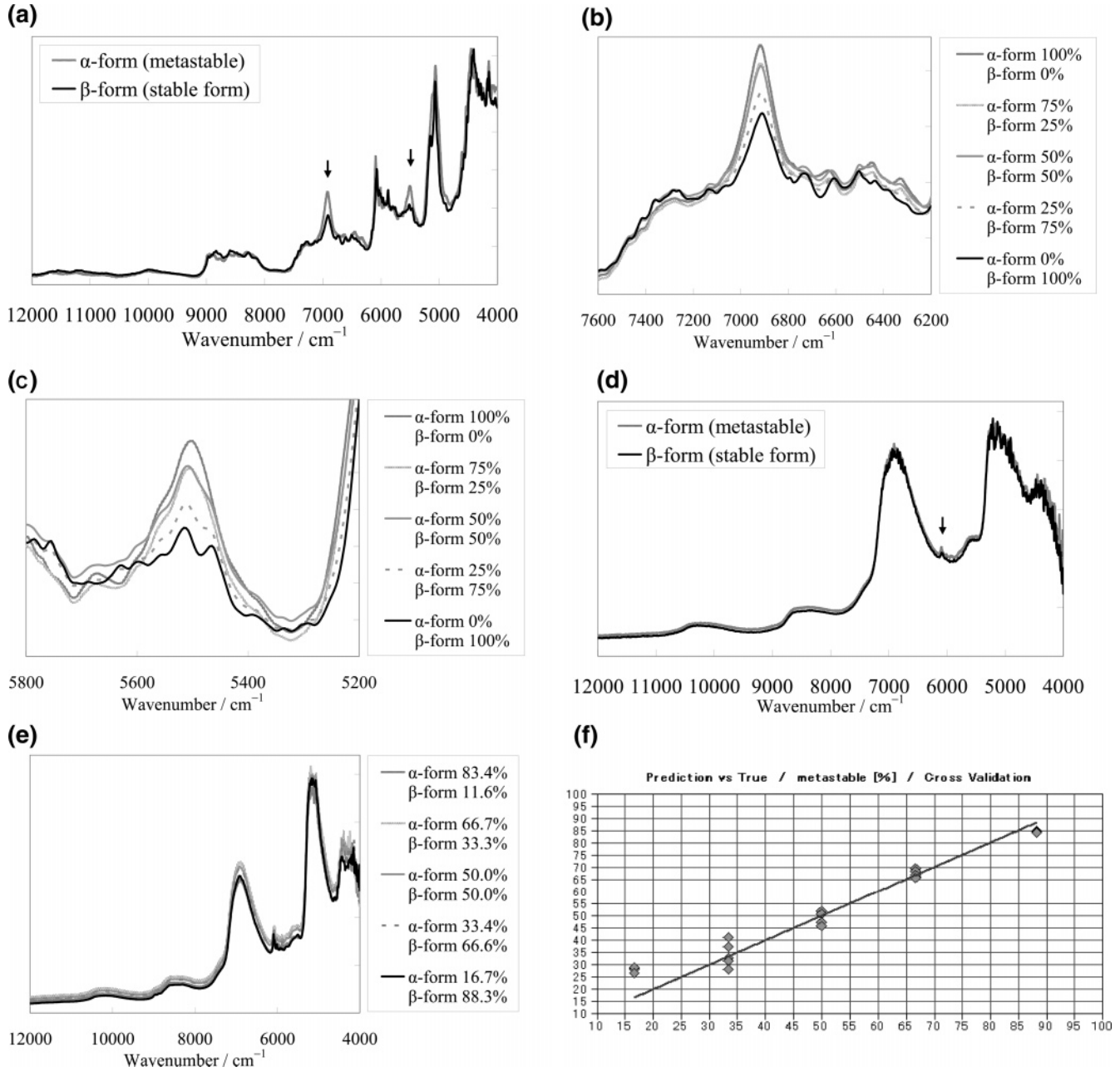


***Figure 6.*** **(a) NIR spectra of timepidium bromide (powder) in the region of 12000−4000 cm$^{-1}$. (b) Enlarged portion of a (timepidium bromide (powder), 7600−6200 cm$^{-1}$). (c) Enlarged portion of a (timepidium bromide (powder), 5800−5200 cm$^{-1}$). (d) NIR spectra of timepidium bromide in slurry in the region of 12000−4000 cm$^{-1}$. (e) NIR spectra of timepidium bromide in slurry with variable concentrations in the region of 12000−4000 cm$^{-1}$. (f) Analytical curve of NIR spectra of timepidium bromide in slurry in the region of 6200−5500 cm$^{-1}$. Determination coefficient ($R^2$) was 94.4% (RMSECV = 5.92, rank = 2).**

5a. With this finding, the monitoring of the polymorphic transition is a distinct possibility.

*A.2.2. Analysis of Timepidium Bromide.* NIR spectra of timepidium bromide (powder) are shown in Figure 6a. The intensities of specific peaks at 7000 and 5500 cm$^{-1}$ are changed, and the differences between the polymorph forms can be easily identified by observing these peaks. It was also considered that the spectral changes were based on the transformation from dihydrate to monohydrate accompanying the polymorphic transition of timepidium bromide, because the intensity ratios of these peaks were proportional to the mixture ratios of the α- and *β*-forms. Therefore, it was considered that these peaks could be assigned to the water molecule in the timepidium bromide crystal. Enlarged portions of Figure 6a are shown in Figure 6b (7000 cm$^{-1}$) and Figure 6c (5500 cm$^{-1}$). The peak at 7000 cm$^{-1}$ is equivalent to the absorption band of the first overtone of water. On the other hand, the peak at 5500 cm$^{-1}$ is not assigned to a vibrational structure because it deviates from the absorption bands corresponding to the molecular structures of timepidium bromide and water. On the basis of the fact that the intensities of the peaks at 5500 cm$^{-1}$ in the two forms change according to the water contents, they could be considered as peaks due to water bound within the crystalline lattice.

The NIR spectra of timepidium bromide (concentration of about 10 w/w) in a slurry are shown in Figure 6d. The

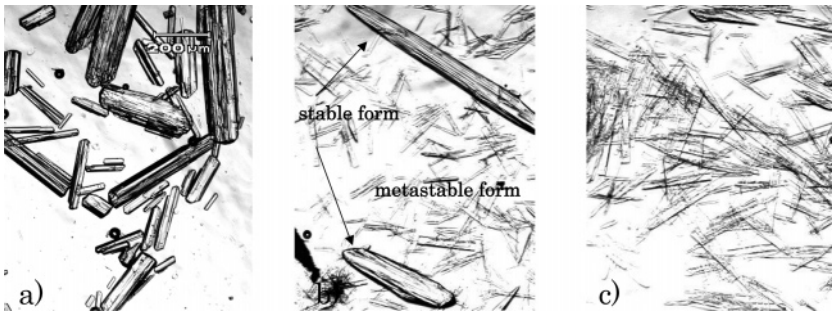


***Figure 7.*** **Polymorphic transition of taltirelin. (a) Before transition (stable form); (b) halfway through transition; (c) after transition (metastable form). Almost all the short particle diameters of the metastable forms are less than 20 $\mu$m.**

entire spectrum region is covered with the absorption band of water. However, a small peak is observed at 6000 $cm^{-1}$. This region corresponds to the first overtone of the CH bonding, and it was considered that the peak is due to the molecule structure of timepidium bromide. A PLS regression analysis of the spectra (based on the peak (6200−5900 $cm^{-1}$)) with various combinations of the α- and $\beta$-forms was performed . However, no correlation was observed between the peak intensities and the ratios of the polymorphic crystal forms. (Determination coefficient ($R^2$) was always under 10%.)

On the other hand, because a clear correlation was observed between the peak intensities and the polymorphic form ratios in the case of the powder state experiment (determination coefficient ($R^2$) = 98.59%, RMSECV = 4.2, rank = 1), it was suggested that the slurry concentration was too low in the previous case to observe any correlation under these experimental conditions. Thus, the polymorphic transition was monitored using a higher concentration (100 w/w%), as shown in Figure 6e. The peaks at 7000 and 5500 $cm^{-1}$ were covered with the absorption band of water, and no correlation is observed between the peak intensities and the ratios of the crystal forms. However, the results of PLS regression analysis on the domain containing the specific peak at 6000 $cm^{-1}$ reveal a strong correlation between the peak change and crystal form (Figure 6f). Therefore, the possibility of monitoring polymorphic transition in a highly concentrated slurry was verified.

**B. Application of Raman and NIR Spectroscopy to In-LineCrystallization Monitoring.** Owing to the absence of water peak interference, the monitoring of the polymorphic transitions in the two compounds by Raman spectroscopy was performed successfully. The trends of the Raman signals yielded information regarding the kinetics of the polymorphic transition, which are important parameters from the viewpoint of manufacturing scale-up. In situ monitoring by Raman spectroscopy was useful for determining the endpoint of the polymorphic transition as well as for understanding the phenomenon.

On the other hand, it was difficult to monitor polymorphic transition by NIR spectroscopy because the NIR spectra were covered by numerous absorption bands of water in the case of a slurry with a low concentration. In the case of a highly concentrated slurry, the monitoring of the polymorphic transition is a distinct possibility but the accuracy is lower than that with Raman.

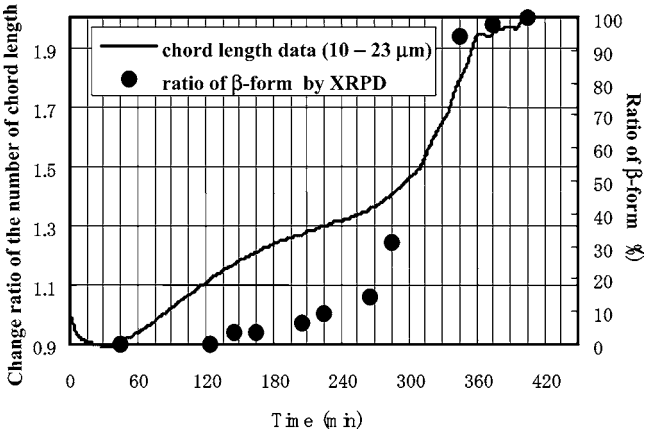


***Figure 8.*** **Line of the chord length data (10−23 $\mu$m) shows the increase in the number of fine particles of the $\beta$-form (stable form). The solid circles represent the ratios of the $\beta$-form determined by powder X-ray diffraction.**

From these results, it is evident that Raman spectroscopy is more effective than NIR spectroscopy for conditions that involve a high degree of interference by water, such as a slurry with a low concentration.

**C. In-line Crystal Shape and Size Monitoring by FBRM.** *C.1. Analysis of Taltirelin (FBRM).* The differences in the crystal shapes of the α- and-$\beta$ forms are recognizable under a microscope (Figure 7). The α-form crystals are prismatic, whereas the $\beta$-form crystals exhibit very small needle-like shapes. Therefore, the transformation from the α-form to the $\beta$-form can be followed through microscopic observations.

Figure 8 shows the trend for the counts of fine chords (10−23 $\mu$m) that correspond to the size of the $\beta$-form. On the addition of the seed to the slurry, a slow rise is observed, which reaches a plateau at 6 h (solid line in Figure 8). This increase is most likely due to the nucleation of the $\beta$-form crystals.

The solid circles represent the ratios of the $\beta$-form, as determined by powder X-ray diffraction (these data were obtained by off-line measurements). The mass fraction of the $\beta$-form does not completely lie on the FBRM curve but levels out in a similar manner at 6 h. The FBRM data show the count of the particles. Therefore, the trend of the fine chords is more strongly emphasized than that of the coarse chords. In the case of taltirelin, the $\beta$-form is extremely small as compared to the α-form. Therefore, FBRM should be available for detection of the start on polymorphic transition.

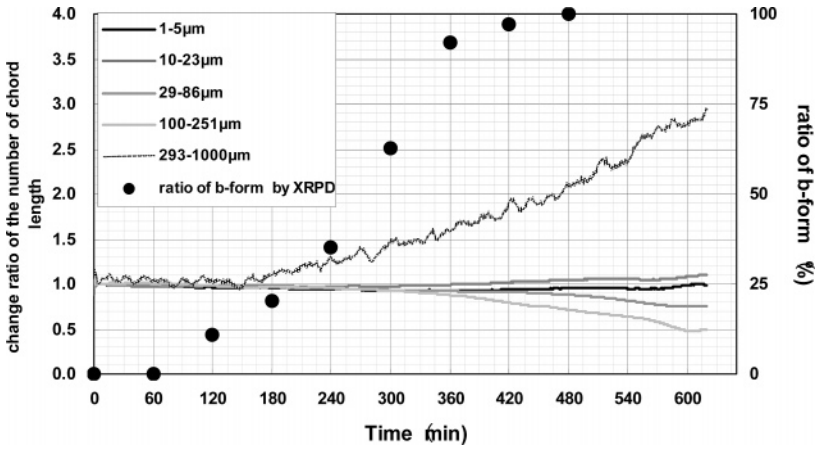


***Figure 9.*** **Each line of the chord length data shows the change in the number of each chord length. The solid circles represent the ratios of the $\beta$-form determined by powder X-ray diffraction. These changes in the number of chord lengths are not in agreement with a polymorphic transition.**

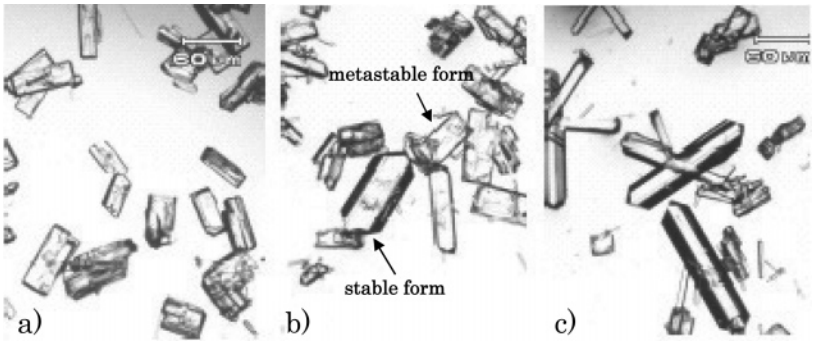


***Figure 10.*** **Polymorphic transition of timepidium bromide. (a) Before transition (stable form); (b) halfway through transition; (c) after transition (metastable form).**

*C.2. Analysis of Timepidium Bromide (FBRM).* Figure 9 shows the changes in the measured chord length data. The data are divided into five population ranges: 1−5 $\mu$m, 10−23 $\mu$m, 29−86 $\mu$m, 100−251 $\mu$m, and 293−1000 $\mu$m. The change ratios of the number of the chord length (the value at seeding is assumed to be 1) are not in agreement with the polymorphic transition. The difference in the crystal shapes of the $\alpha$- and $\beta$-forms was confirmed by examining a micrograph (Figure 10). The $\alpha$-form crystal showed a thin plate shape, whereas the $\beta$-form crystal was prismatic in shape. However, the difference between the chord lengths of the two forms was small.

In the case of timepidium bromide, it was difficult to monitor the transition from the $\alpha$-form to the $\beta$-form by FBRM. Since the difference in the particle size of the two forms was small, no spectral difference was detected between them.

**D. Application of FBRM to In-line Crystallization Monitoring.** In order to consider FBRM as a PAT tool for monitoring polymorphic transition, it is necessary to investigate the relationship between crystal habit and polymorphism.

A polymorphic transformation is often accompanied by a change in the crystal habit, which can cause changes in the particle distribution measured by FBRM. In this case, FBRM can prove very useful as a PAT tool for monitoring not only particle distribution size but also polymorphic transition.

## Conclusion

We used three independent techniques to monitor polymorphic transitions.

**1. Raman Spectroscopy.** In the case of timepidium bromide, the ratio of polymorphic forms can be determined by PLS regression analysis. In addition, in situ monitoring of polymorphic transition was successfully carried out in both compounds because the spectra did not show any interference from water. However, it was considered that the monitoring might be difficult with other crystalline forms having complicated Raman spectra.

**2. NIR Spectroscopy.** Measurements on the polymorphic forms were difficult under the experimental conditions in a slurry. However, an attempt was made to distinguish between the polymorphic forms and their ratios in the case of the powder state and highly concentrated slurry. The monitoring of polymorphic transition might be possible, depending on the conditions such as highly concentration slurry.

**3. FBRM.** Although very useful as a PAT tool for monitoring not only particle distribution size but also multiform transition, FBRM can be employed only when the particle distribution size changes with polymorphic transition.

Under these conditions, Raman and NIR spectroscopy were verified to be in some care suitable as PAT tools for carrying out the monitoring of a polymorphic transition during crystallization. In particular, in situ Raman spectroscopy can assist in the understanding of the kinetics of poly-

morphic transition during crystallization and can be used to develop a robust process and determine the endpoint. Furthermore, this study demonstrated the possibility of using FBRM for monitoring the polymorphic transition process, depending on the relationship between crystal habit and polymorphism; it was shown that FBRM is an attractive prospect because it can function as a sensitive in situ tool.

We obtained the necessary knowledge for developing and monitoring a process without sampling work or the risk of contamination by in situ techniques (Raman, NIR, andFBRM), which are demonstrated as promising tools for detecting kinetics in the pharmaceutical crystallization industry.


## Acknowledgment

We thank Mr. M. Yamada of S.T. Japan Inc. for the use of the Raman spectroscope and the Japan Health Sciences Foundation for financial support (KH31029).

Received for review February 27, 2006.

OP060046Y